

## Supplementary Information

### Light Upconversion by Triplet-Triplet Annihilation in Diphenylanthracene-Based Copolymers

*Soo-Hyon Lee, Mathieu A. Ayer, Roberto Vadrucci, Christoph Weder\*, and Yoan C. Simon\**

Adolphe Merkle Institute, University of Fribourg, Route de l'Ancienne Papeterie, P.O. Box 209,  
CH-1723 Marly 1, Switzerland

E-mails: christoph.weder@unifr.ch; yoan.simon@unifr.ch

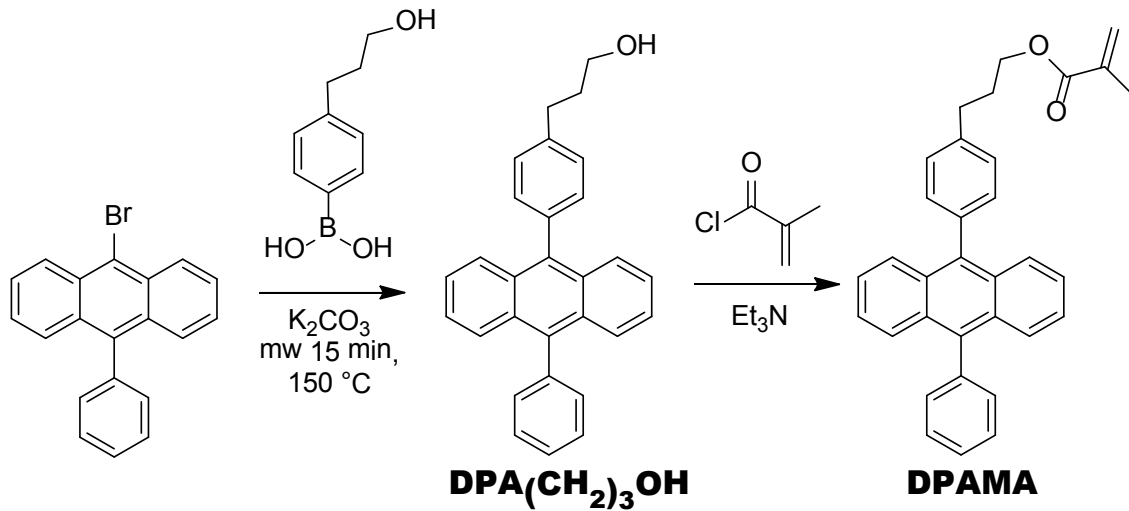
### Table of Contents

I.	Synthesis and characterization	S2-S6
II.	$^1\text{H}$ and $^{13}\text{C}$ NMR spectra and polymer composition	S7-S15
III.	Thermal studies	S16-S20
IV.	Thin film studies	S21-S26
V.	Morphological characterization	S23-S25
VI.	Optical measurements	S26-S31

## I. Synthesis and Characterization

**Materials.** All chemicals were purchased from Sigma-Aldrich except 4-(3-hydroxypropyl) benzeneboronic acid (96 %, 180.01 g/mol), which was purchased from ABCR GmbH. 2,2'-Azobisisobutyronitrile (AIBN) was purified by recrystallization from methanol prior to use. All other chemicals were used without any further purification. 9-Bromo-10-phenylanthracene was synthesized as previously reported.<sup>1</sup> Microwave-assisted syntheses were performed with a Biotage® Initiator Microwave Synthesizer and all purification steps were performed by flash column chromatography (FCC) using a Biotage® IsoleraOne<sup>TM</sup>. Polymers were analyzed with gel permeation chromatography (GPC) equipped with PSS SECcurity injector, two PSS SDV linear M columns (dimension 8 x 300 mm, particle size 5 micrometers) and Agilent 1260 MDS Refractive Index Detector using GPC grade tetrahydrofuran (THF) as an eluent with 250 ppm BHT as inhibitor at a flow rate of 1 mL/min.

**Scheme S1** Synthesis of the DPA-containing monomer DPAMA.



**3-[4-(10-Phenylanthracen-9-yl)phenyl]propan-1-ol (DPA( $\text{CH}_2$ )<sub>3</sub>OH).** In a microwave tube, 9-bromo-10-phenylanthracene (1.25 g, 3.7 mmol, 1 eq.), 4-(3-hydroxypropyl) benzeneboronic acid (0.74 g, 4 mmol, 1.1 eq.) and  $\text{K}_2\text{CO}_3$  (3 g, 21.7 mmol, 6 eq.) were suspended in a mixture of

benzene (10 mL) and H<sub>2</sub>O (5 mL). The slurry was purged with argon for 15 min and Pd(PPh<sub>3</sub>)<sub>4</sub> (21 mg, 0.017 mmol, 0.005 eq.) was then added to the mixture. The vessel was sealed and placed in the microwave synthesizer. After 2 min of pre-stirring, the content was heated to 150 °C at a pressure of 3 bar for 15 min, and cooled down to 50 °C. The suspension was then filtered through a fritted glass filter and the grey precipitate was washed with dichloromethane (DCM, 5 mL). DCM (10 mL) was added to the filtrate and the organic phase was extracted with brine (2 x 25 mL) and water (2 x 25 mL). The organic layers were collected and concentrated in vacuo. The crude solid was then purified by FCC (hexane:DCM = 3:1, R<sub>f</sub> = 0.35). A light yellowish solid was obtained in a yield of 65 % (930 mg); <sup>1</sup>H NMR (360 MHz, CD<sub>2</sub>Cl<sub>2</sub>, δ): 1.43 (s, 1H, OH), 1.99-2.04 (quintet, 2H, CH<sub>2</sub>), 2.85-2.89 (t, 2H, CH<sub>2</sub>OH), 3.74-3.76 (q, 2H CH<sub>2</sub>Ar,), 7.30-7.70 ppm (m, 17H, Ar); <sup>13</sup>C NMR (90 MHz, CD<sub>2</sub>Cl<sub>2</sub>, δ): 32.67, 35.03, 62.49, 125.10, 125.68, 127.18, 127.60, 128.28, 129.19, 129.26, 130.45, 130.66, 131.89, 132.02, 137.26, 137.80, 138.10, 139.33, 141.98 ppm; mp: 213.5 °C; MALDI-TOF MS *m/z*: 388.20 [M<sup>+</sup>] (calculated molar mass: 388.18 g/mol).

**3-[4-(10-Phenylanthracen-9-yl)phenyl]propyl methacrylate (DPAMA).** In a 250 mL two-necked round-bottom flask under argon, DPA(CH<sub>2</sub>)<sub>3</sub>OH (0.9 g, 2.3 mmol, 1 eq.) and triethylamine (0.48 mL, 3.47 mmol, 1.5 eq.) were dissolved in dry THF (70 mL) and cooled to 0 °C. Methacryloyl chloride (0.34 mL, 3.47 mmol, 1.5 eq.) was added dropwise to the reaction mixture. The solution was allowed to warm up to r.t. and stirred for 1 day. After evaporation of the solvent, the off-white powder obtained was purified by FCC (hexane:ethylacetate = 5:1 elution, R<sub>f</sub> = 0.65) in a yield of 60 % (630 mg) <sup>1</sup>H NMR (360 MHz, CD<sub>2</sub>Cl<sub>2</sub>, δ): 1.97 (s, 3H, CH<sub>3</sub>), 2.14-2.20 (quintet, 2H, CH<sub>2</sub>), 2.88-2.92 (t, 2H, CH<sub>2</sub>O), 4.25-4.28(t, 2H, CH<sub>2</sub>Ar), 5.59 (s, 1H, CH<sub>2</sub>=CH<sub>2</sub>) 6.13 (s, 1H, CH<sub>2</sub>=CH<sub>2</sub>), 7.30-7.69 ppm (m, 17H, Ar); <sup>13</sup>C NMR (90 MHz, CD<sub>2</sub>Cl<sub>2</sub>, δ): 18.42, 30.63, 32.25, 64.10, 125.17, 125.22, 125.33, 126.96, 127.08, 127.75, 128.65,

128.79, 130.03, 130.18, 131.51, 136.72, 136.95, 137.23, 137.36, 139.26, 141.03, 167.55 ppm;  
m.p: 123 °C; MALDI-TOF MS  $m/z$ : 456.21 [M<sup>+</sup>] (calculated molar mass: 456.21 g/mol).

**General procedure for the synthesis of poly(DPAMA-*co*-MMA) by free radical polymerization.** Example for polymer **2** In a 5 mL Schlenk tube under argon, MMA(296.04 mg, 2.96 mmol), DPAMA(450 mg, 0.99 mmol), and recrystallized AIBN(1.08 mg, 0.0066 mmol) were dissolved in dry toluene (2 mL). After degassing under argon for 30 min in an ice bath, the mixture was placed in a pre-heated oil bath at 70 °C and the reaction was allowed to proceed at this temperature for 5 h. The content of the tube was subsequently precipitated dropwise into 200 mL of r.t. methanol. A solid polymer was collected after centrifugation at 3500 rpm for 15 min with a yield of 55 %. The composition of copolymers was determined by <sup>1</sup>H NMR spectra by comparing the integrations of the benzylic protons of DPAMA at  $\delta$  = 4.0 ppm with the ester protons of both DPAMA and MMA at  $\delta$  = 3.5 ppm (Fig. S6-S10).

**Thermal Studies.** Thermogravimetric analyses (TGA) were performed on a Mettler-Toledo TGA STAR instrument by heating the (co)polymer from 25 °C to 500 °C under nitrogen (N<sub>2</sub>) at 10 °C/min (Fig. S17). Differential scanning calorimetry (DSC) experiments were performed on Mettler-Toledo STAR DSC instrument by heating the samples from 25 °C to 220 °C, cooling from 220 °C to 0 °C, and heating again to 250 °C under N<sub>2</sub> atmosphere. All experiments were conducted with heating or cooling rates of 10 °C/min (Fig. S18-S23). The glass transition temperatures ( $T_g$ ) of the (co)polymers measured by DSC on second heating cycle with heating rate of 10 °C/min were compared to the  $T_g$  calculated by the Fox and Flory equation (Equation 1, Fig. S24).<sup>2</sup>

**Materials processing.** *Method A:* Solution casting. Poly(DPAMA-*co*-MMA) (30 mg) and PdOEP (0.05 wt%) were dissolved in ~1 mL of toluene. The solution mixture was drop-cast onto

a glass slide and the solvent was evaporated at 50 °C in a vacuum oven (0.05 bar) for 2 days. The resulting films were used directly for subsequent photoluminescence analysis. The thickness of the resulting films, measured using a digital caliper (Millimess Inductive Digital comparator extramess 200, Mahr) was between 80-193 µm (Table S1).

*Method B:* Compression molding. Poly(DPAMA-*co*-MMA) (30 mg) and PdOEP (0.03 %, 0.05 % and 0.18 wt%) were dissolved in ~1 mL of toluene. The solution mixture was drop-cast onto a glass slide, and the solvent was evaporated at 105 °C by placing the glass slide onto a hot plate. The resulting film was covered with a second glass slide and placed in a Carver® press at 160 °C applying light pressure. After compression-molding for 5 min, the films were delaminated from the glass slides and their thickness, measured using the aforementioned caliper, was between 110 and 245 µm. (Table S1).

*Method C:* Spin-coating. Poly(DPAMA-*co*-MMA) (10 mg) dissolved in DCM (0.5 mL) was drop-cast and spin-coated onto a glass slide at 2500 rpm for 3 min. The thicknesses of the thin films were determined by scratching the samples with a razor blade and measuring the depth using a JPK Nanowizard II atomic force microscope (AFM) with a SPM Controller III in air and tapping mode (AC mode) with a silicon nitrate tip cantilever (Nominal spring constant of 40 N/m and resonance frequency of 300 kHz) and the recorded thicknesses varied between 500-600 nm (Fig. S25).

**Optical Experiments.** The UV-Vis absorption and conventional photoluminescence spectra of the (co)polymers were determined on films that were prepared by spin-coating (*Method C*). The optical absorption spectra of the resulting thin films were recorded with a Shimadzu UV-2401PC UV-vis spectrophotometer. Their fluorescence spectra were measured by excitation at 370 nm

using a solid sample geometry in which the emission was detected (at an angle of 90 ° from the incident light) with a spectrofluorometer from Photon Technology International.

Upconverted fluorescence emission was measured in air by exciting the upconverting films mounted on glass slides prepared by solution-casting (*Method A*) and compression-molding (*Method B*) at 543 nm with a green HeNe laser (2.0 mW, 320 mW/cm<sup>2</sup>) from Thorlabs, and recording emission spectra. A green HeNe line filter at 543 nm from Thorlabs was used to ensure monochromatic excitation at 543 nm. The upconverting films were placed in a solid state sample holder at a 40 ° angle from the laser excitation source and detection was recorded at 90 ° from the incident light. The power dependence of the upconverted fluorescence versus excitation intensity was explored by varying the excitation intensity between 0.2 and 1.26 mW (measured with a power meter PM 100USB from Thorlabs) using a series of neutral density filters to attenuate the transmission from the HeNe laser.

**Small-angle X-ray scattering (SAXS).** The spectrum was obtained by using a NanoMax-IQ camera (Rigaku Innovative Technologies, Auburn Hills, MI USA). The sample was kept at room temperature in vacuum during the measurements. Raw data were processed according to standard procedures, and the isotropic scattering spectrum is presented as a function of the momentum transfer  $q = 4\pi \cdot \lambda^{-1} \cdot \sin(\theta/2)$ , where  $\theta$  is the scattering angle and  $\lambda = 0.1524$  nm is the photon wavelength.

## II. $^1\text{H}$ and $^{13}\text{C}$ NMR spectra and polymer composition

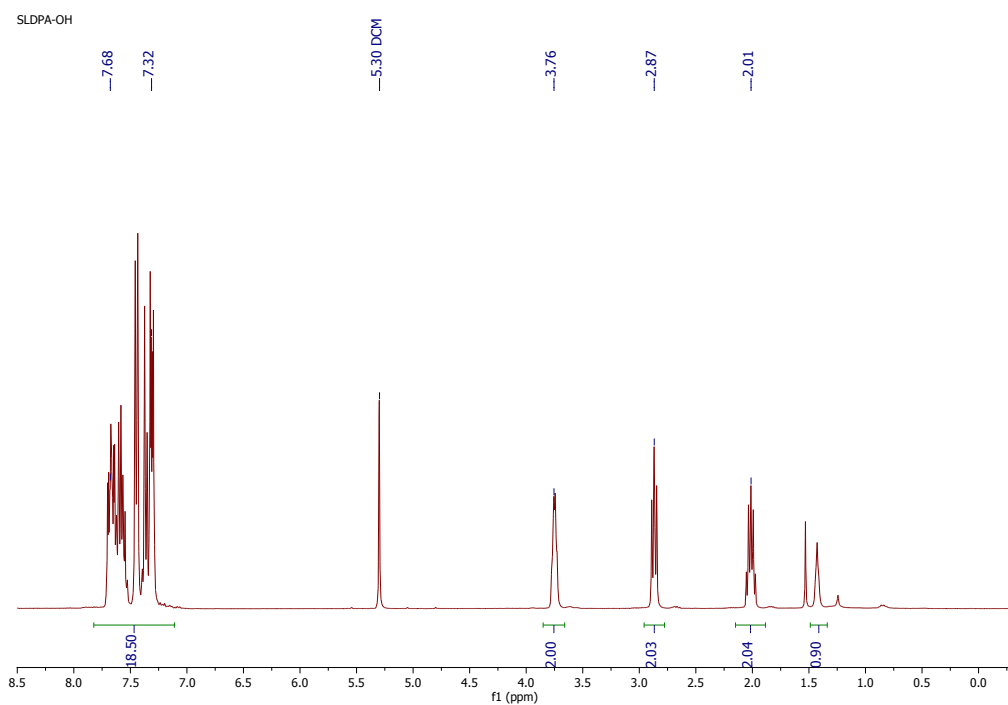


**Fig. S1**  $^1\text{H}$  NMR spectrum (360 MHz,  $\text{CD}_2\text{Cl}_2$ ) of  $\text{DPA}(\text{CH}_2)_3\text{OH}$ .

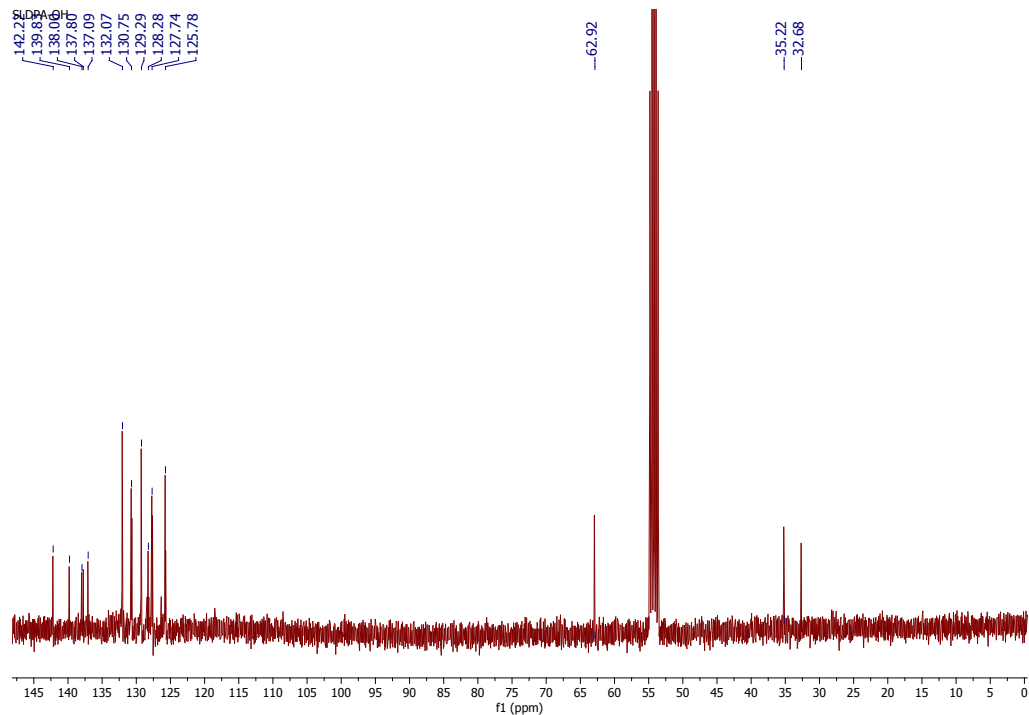


**Fig. S2**  $^{13}\text{C}$  NMR spectrum (90 MHz,  $\text{CD}_2\text{Cl}_2$ ) of  $\text{DPA}(\text{CH}_2)_3\text{OH}$ .

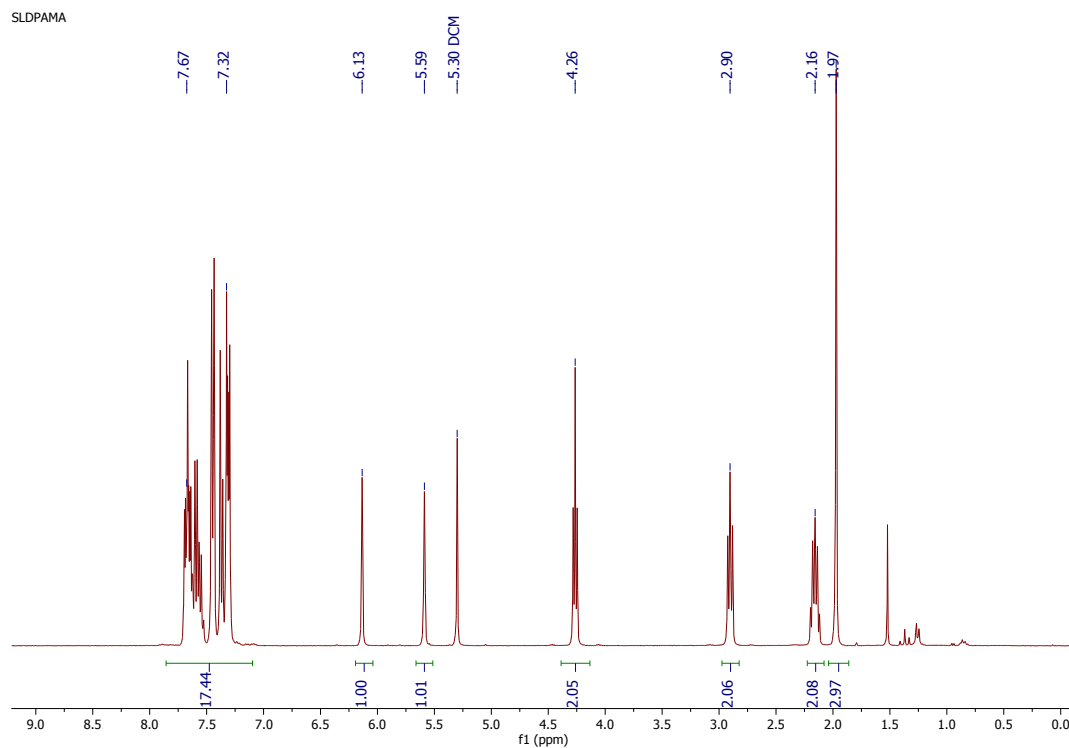


**Fig. S3** <sup>1</sup>H NMR spectrum (360 MHz, CD<sub>2</sub>Cl<sub>2</sub>) of DPAMA.

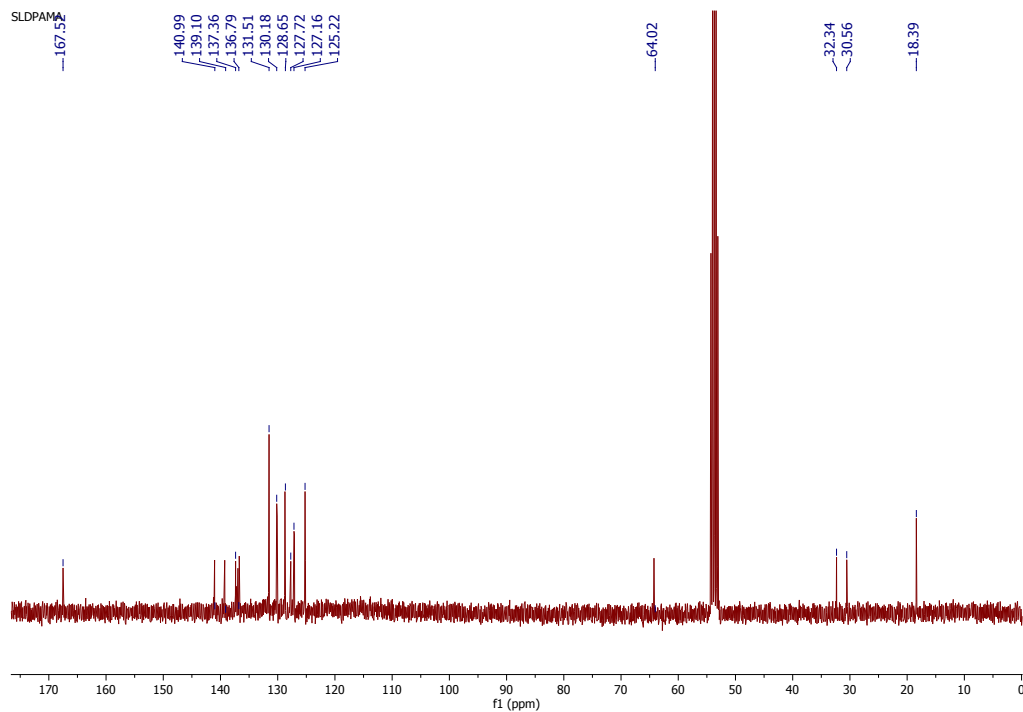


**Fig. S4** <sup>13</sup>C NMR spectrum (90 MHz, CD<sub>2</sub>Cl<sub>2</sub>) of DPAMA.

The DPAMA/MMA ratio in the copolymers (**2-6**) was determined by  $^1\text{H}$  NMR spectroscopy by comparing integrals of the benzylic protons of DPAMA at  $\delta = 4.0$  ppm with the ester protons of both DPAMA and MMA at  $\delta = 3.5$  ppm.

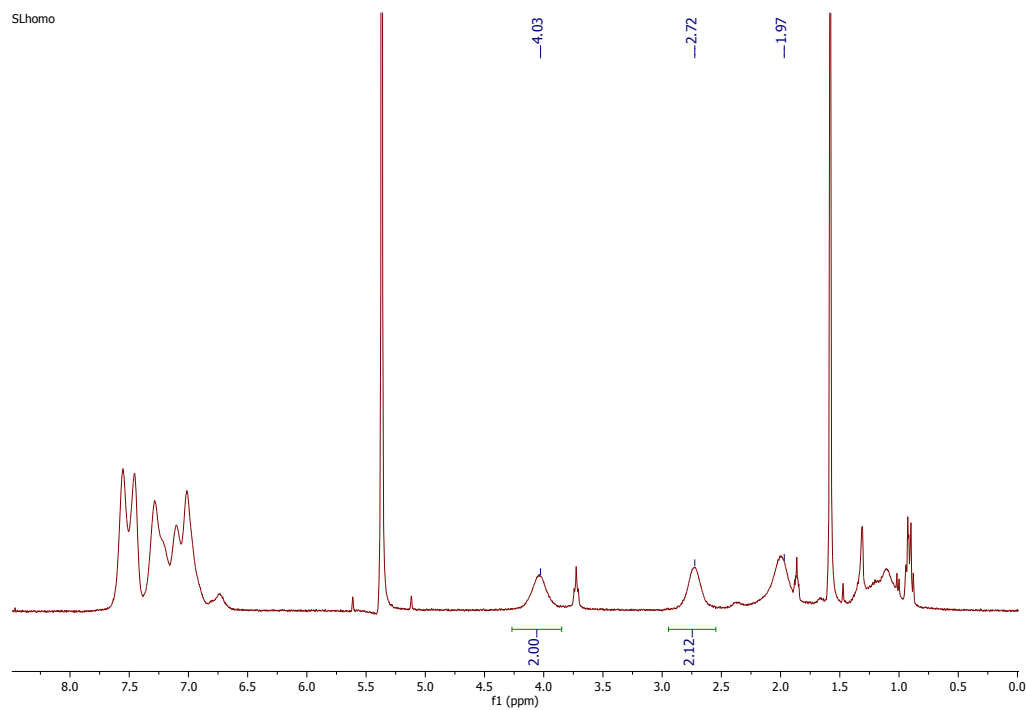


**Fig. S5**  $^1\text{H}$  NMR spectrum (360 MHz,  $\text{CD}_2\text{Cl}_2$ ) of copolymer **1**.

S11-2

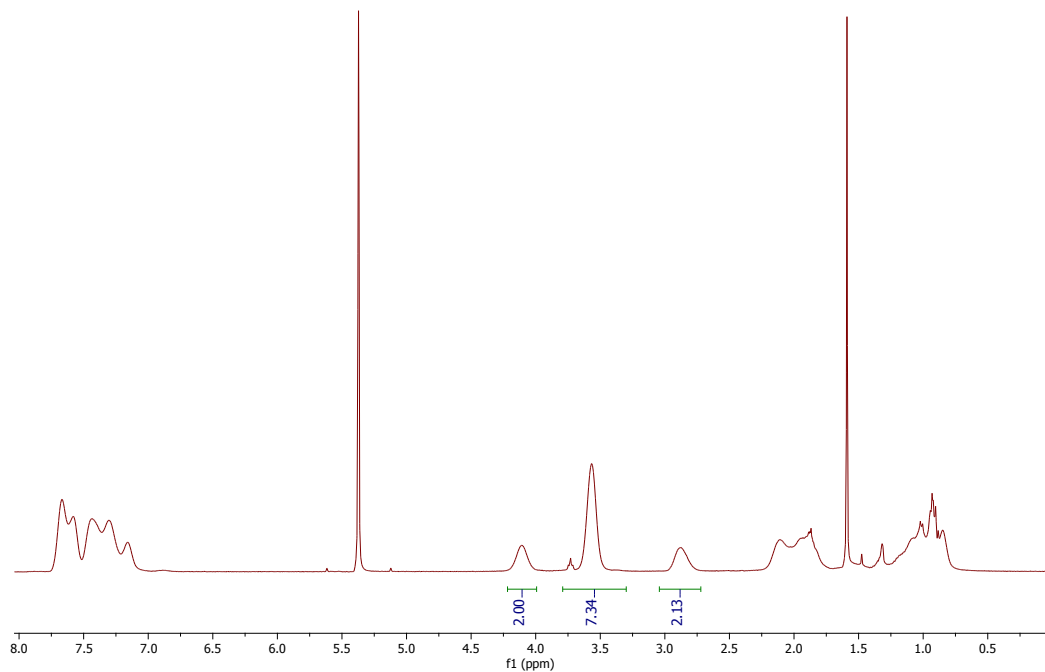


**Fig. S6** <sup>1</sup>H NMR spectrum (360 MHz, CD<sub>2</sub>Cl<sub>2</sub>) of copolymer **2**.

S11-5

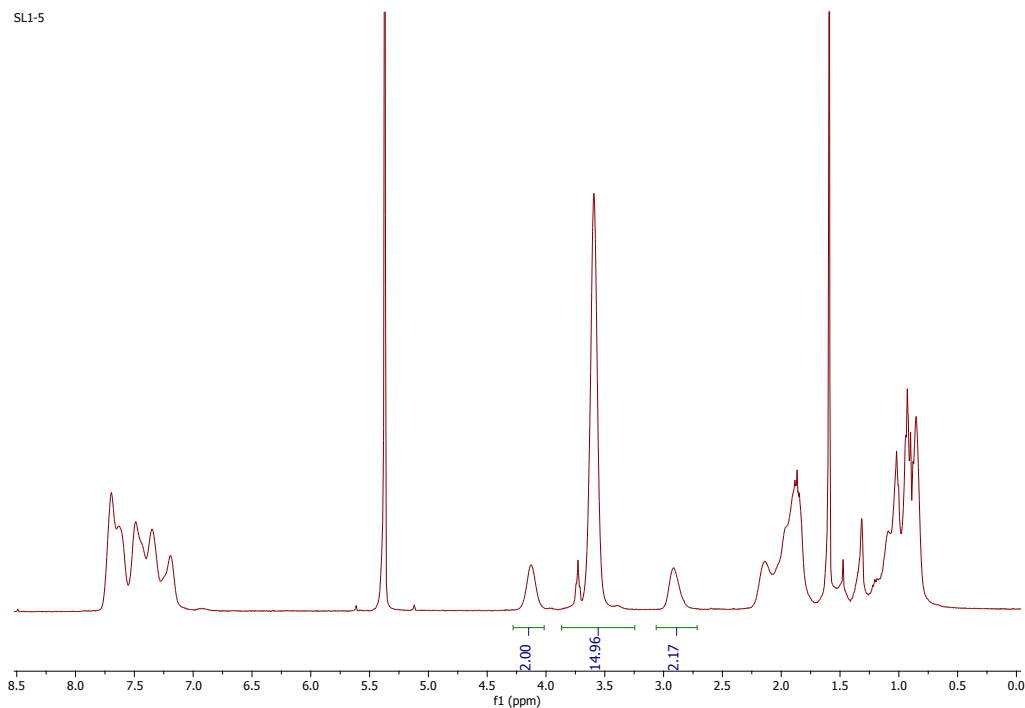


**Fig. S7** <sup>1</sup>H NMR spectrum (360 MHz, CD<sub>2</sub>Cl<sub>2</sub>) of copolymer **3**.

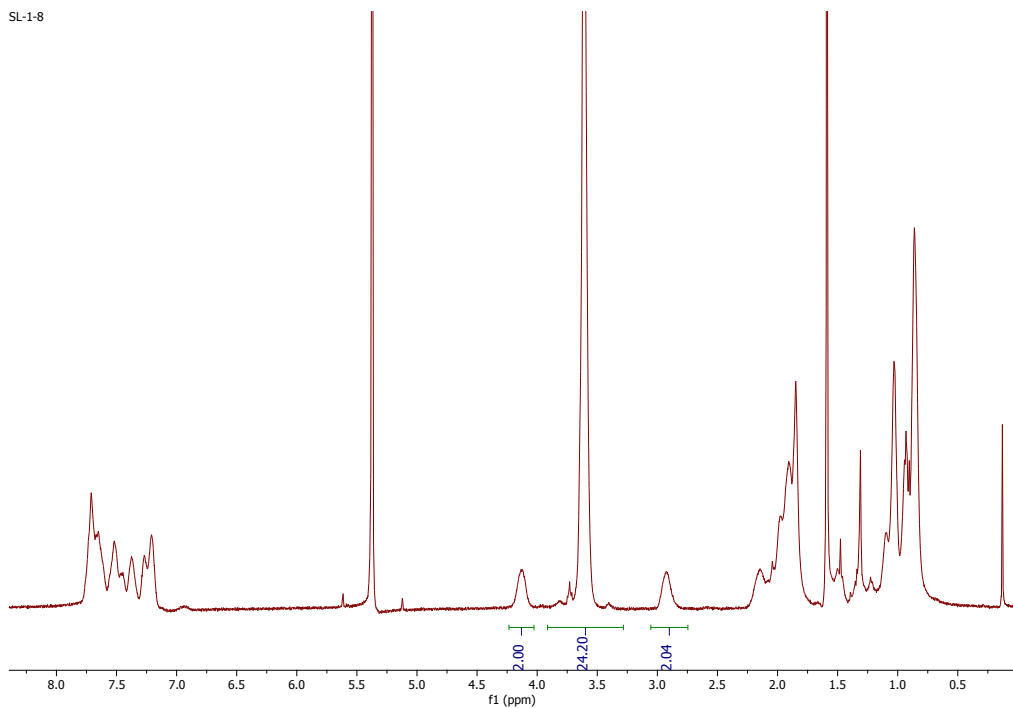


**Fig. S8**  $^1\text{H}$  NMR spectrum (360 MHz,  $\text{CD}_2\text{Cl}_2$ ) of copolymer **4**.

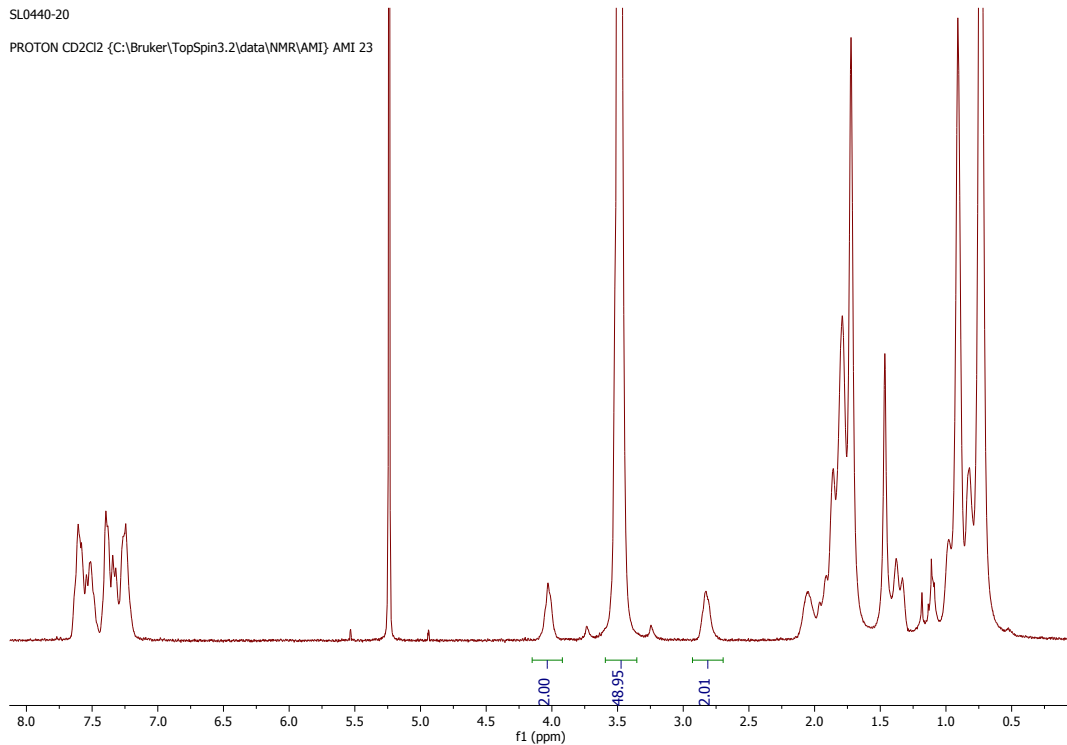


**Fig. S9**  $^1\text{H}$  NMR spectrum (360 MHz,  $\text{CD}_2\text{Cl}_2$ ) of copolymer **5**.

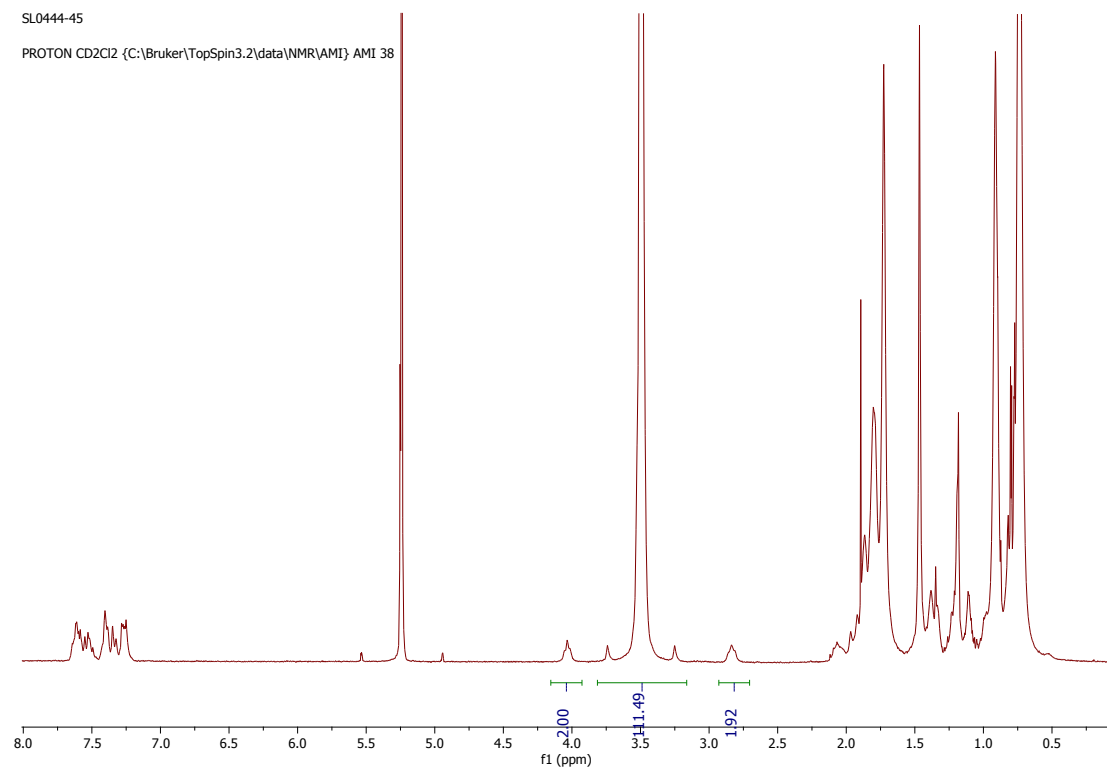


**Fig. S10**  $^1\text{H}$  NMR spectrum (360 MHz, CD<sub>2</sub>Cl<sub>2</sub>) of copolymer **6**.

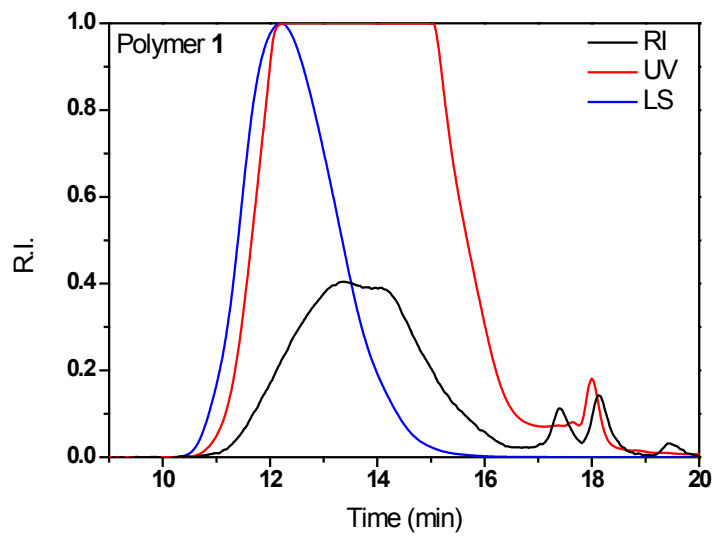


**Fig. S11** Gel permeation chromatogram of polymer **1**.

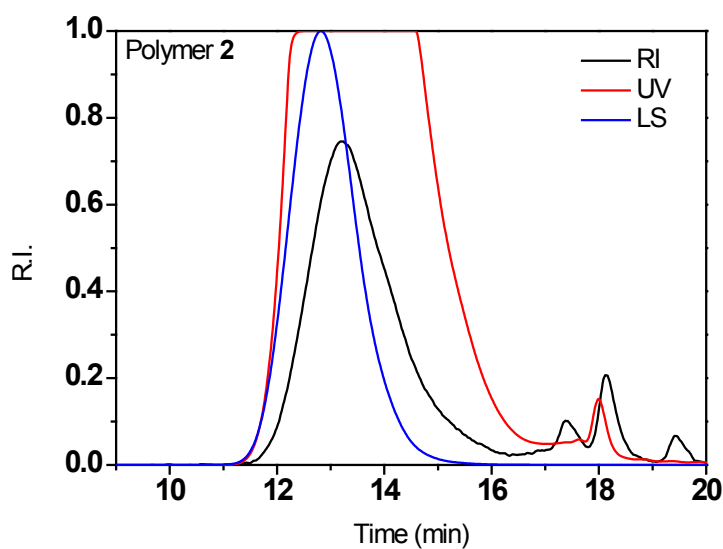


**Fig. S12** Gel permeation chromatogram of polymer **2**.

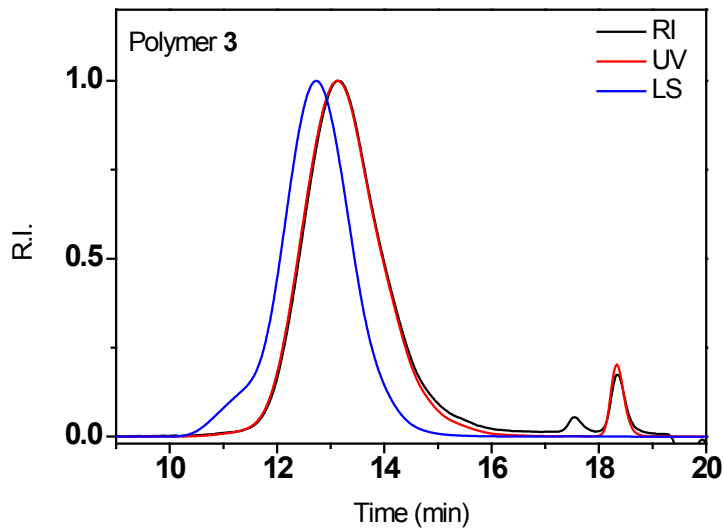


**Fig. S13** Gel permeation chromatogram of polymer **3**.

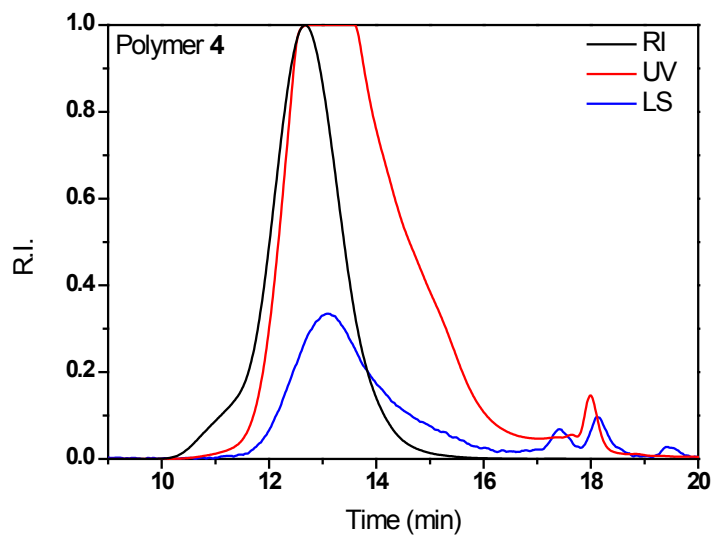


**Fig. S14** Gel permeation chromatogram of polymer 4.

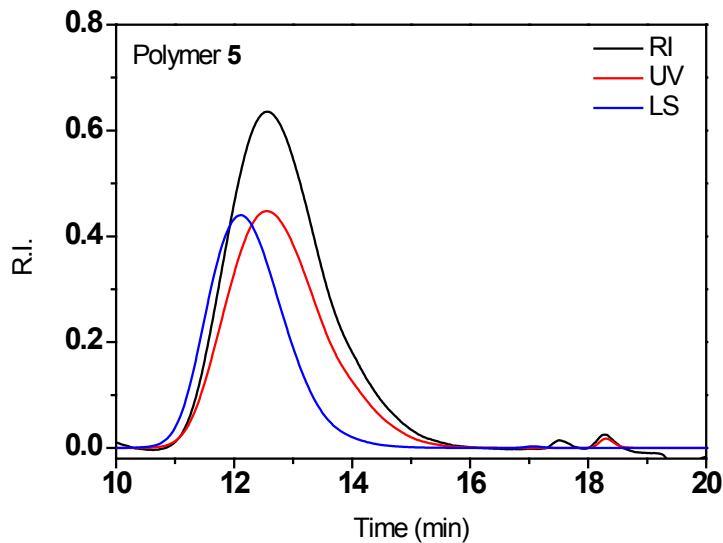


**Fig. S15** Gel permeation chromatogram of polymer 5.

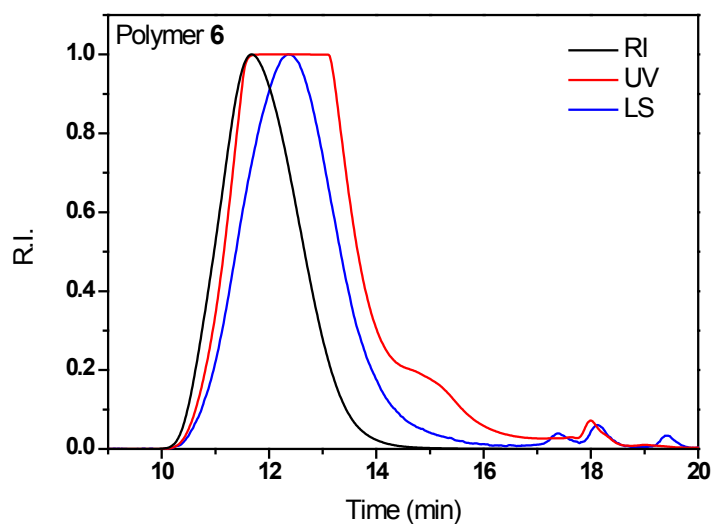


**Fig. S16** Gel permeation chromatogram of polymer **6**.

### III. Thermal studies

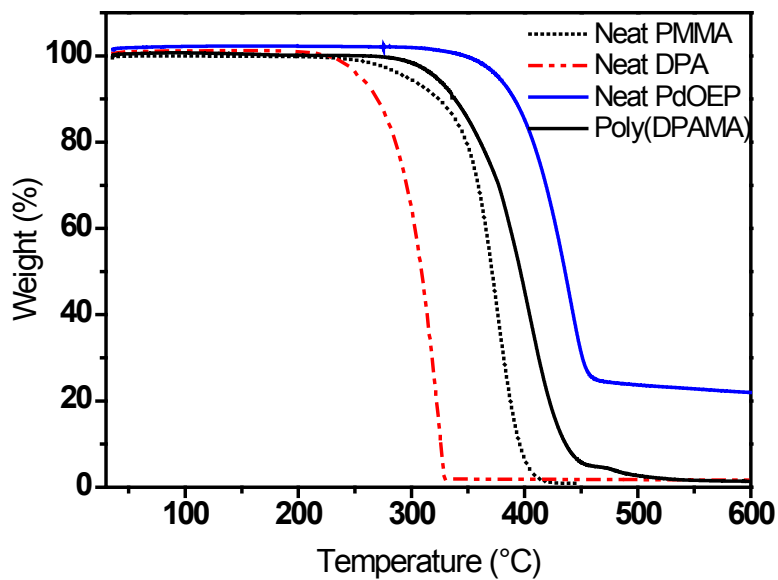


**Fig. S17** Thermogravimetric analysis (TGA) traces of neat PMMA, DPA, PdOEP and DPAMA homopolymer **1**. All experiments were recorded under nitrogen at a heating rate of 10 °C/min.

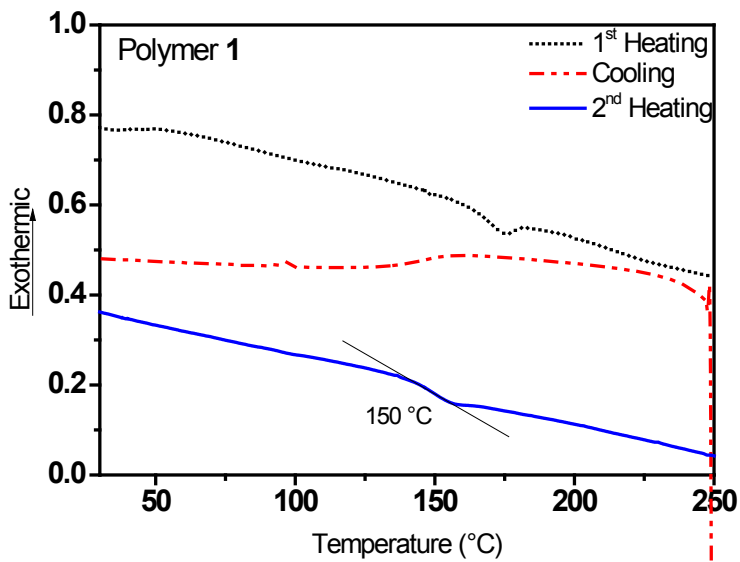


**Fig. S18** Differential scanning calorimetry (DSC) thermograms of homopolymer **1**, recorded under nitrogen. Samples were first heated from 25 °C to 250 °C (black, dotted), cooled from 250 °C to 0 °C (red, dash-dotted), and heated again to 260 °C (blue, solid), all with heating or cooling rates of 10 °C/min.

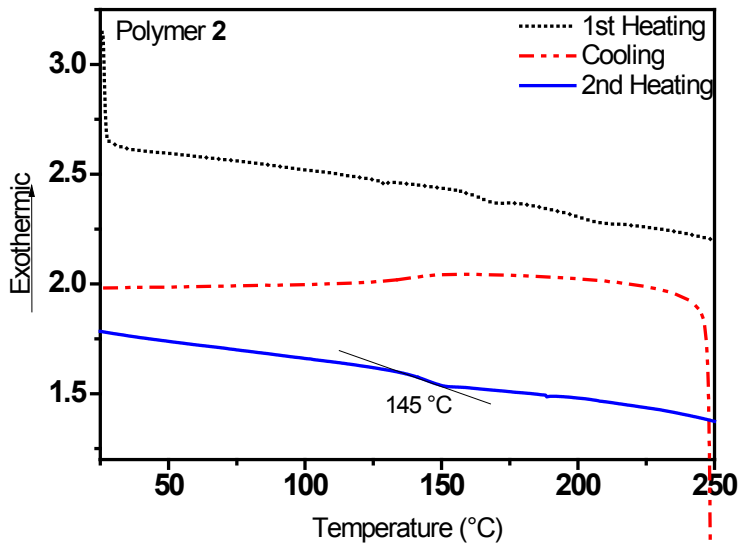


**Fig. S19** Differential scanning calorimetry (DSC) thermograms of copolymer **2**, recorded under nitrogen. Samples were first heated from 25 °C to 250 °C (black, dotted), cooled from 250 °C to 0 °C (red, dash-dotted), and heated again to 260 °C (blue, solid), all with heating or cooling rates of 10 °C/min.

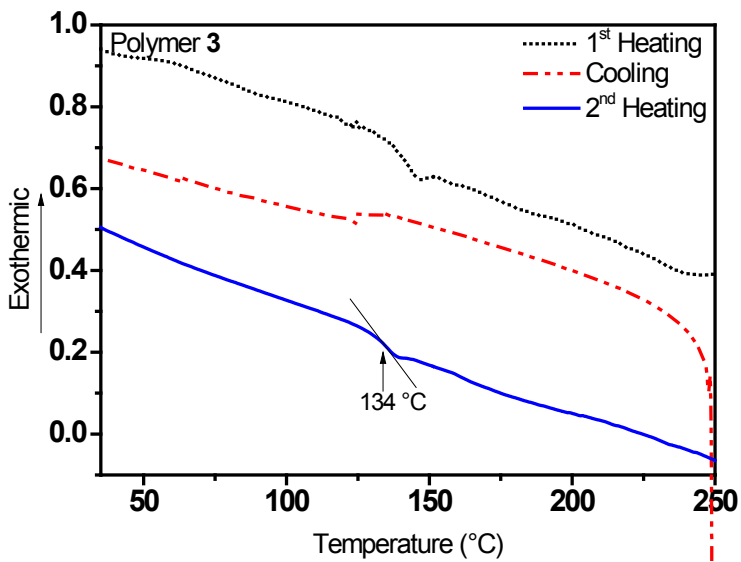


**Fig. S20** Differential scanning calorimetry (DSC) thermograms of copolymer **3**, recorded under nitrogen. Samples were first heated from 25 °C to 250 °C (black, dotted), cooled from 250 °C to 0 °C (red, dash-dotted), and heated again from 0 °C to 260 °C (blue, solid), all with heating or cooling rates of 10 °C/min.

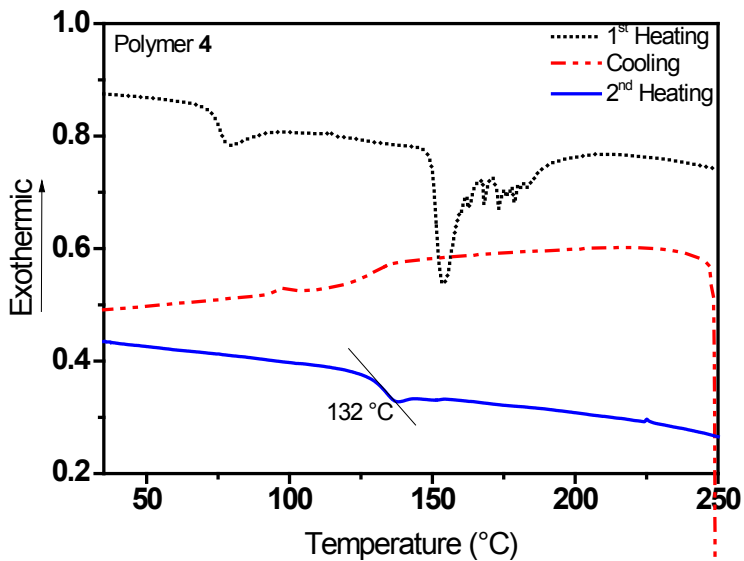


**Fig. S21** Differential scanning calorimetry (DSC) thermograms of copolymer **4**, recorded under nitrogen. Samples were first heated from 25 °C to 250 °C (black, dotted), cooled from 250 °C to 0 °C (red, dash-dotted), and heated again to 260 °C (blue, solid), all with heating or cooling rates of 10 °C/min.

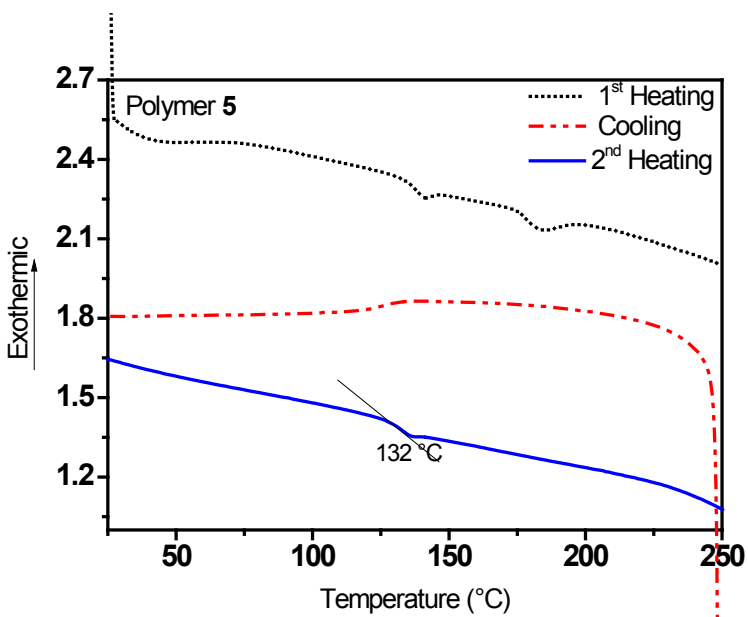


**Fig. S22** Differential scanning calorimetry (DSC) thermograms of copolymer **5**, recorded under nitrogen. Samples were first heated from 25 °C to 250 °C (black, dotted), cooled from 250 °C to 0 °C (red, dash-dotted), and heated again to 260 °C (blue, solid), all with heating or cooling rates of 10 °C/min.

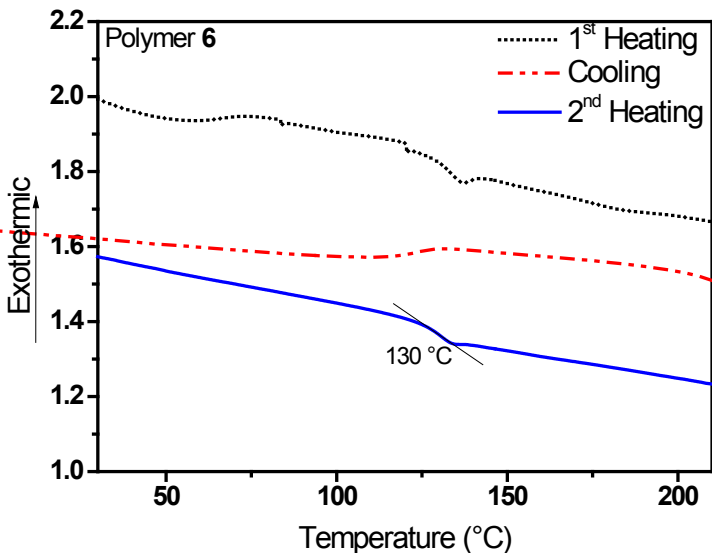


**Fig. S23** Differential scanning calorimetry (DSC) thermograms of copolymer **6**, recorded under nitrogen. Samples were first heated from 25 °C to 250 °C (black, dotted), cooled from 250 °C to 0 °C (red, dash-dotted), and heated again to 260 °C (blue, solid), all with heating or cooling rates of 10 °C/min.

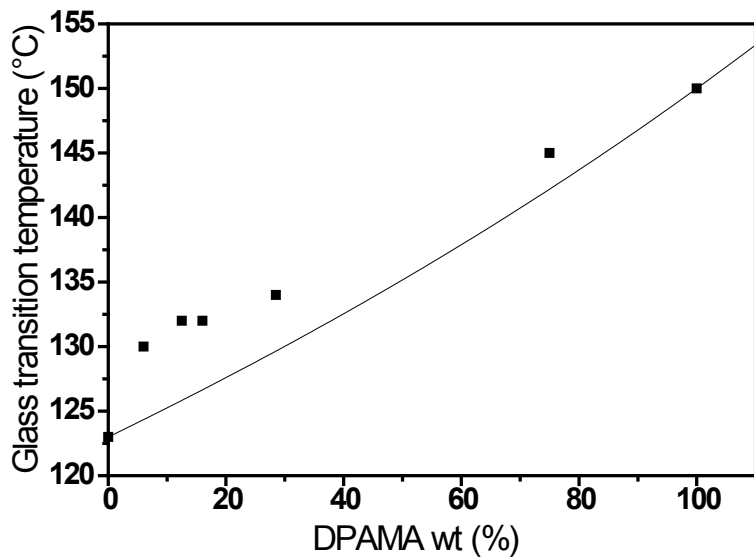


**Fig. S24** Glass transition temperature ( $T_g$ ) of (co)polymers (**1-6**) as a function of weight fraction of DPAMA as measured by DSC (black) and calculated using the Fox equation (red).

Fox equation:

$$\frac{1}{T_g} = \frac{w_A}{T_{gA}} + \frac{w_B}{T_{gB}} \quad \text{Equation S1}$$

#### IV. Thin film studies

**Table S1** Thickness of (co)polymer films containing PdOEP (0.05 wt%) prepared by compression-molding or by solution-casting.

Entry	Film Thickness <sup>a</sup> (μm)	
	Compression-molding	Solution-cast
1	113	136
2	220	193
3	245	134
4	115	65
5	180	55
6	110	138

<sup>a</sup> Thickness was measured with a digital caliper (Millimess Inductive Digital comparator extramess 200, Mahr).

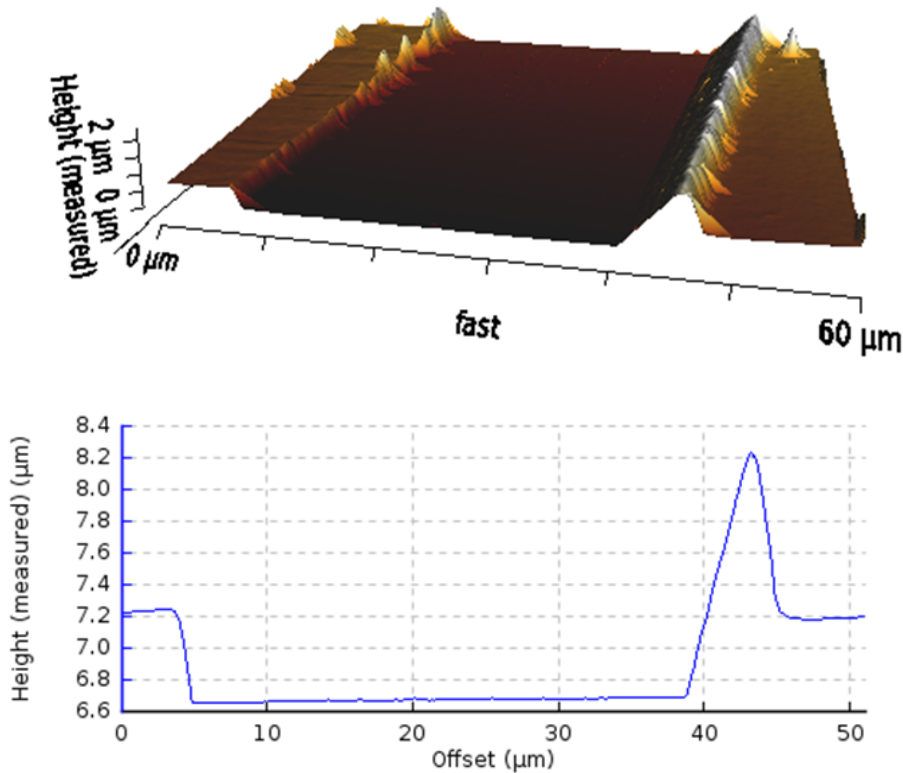


**Fig. S25** Atomic force microscopy (AFM) image of a longitudinal section of the scratched spin-coated DPAMA homopolymer film. The average of its thickness is 600 nm.

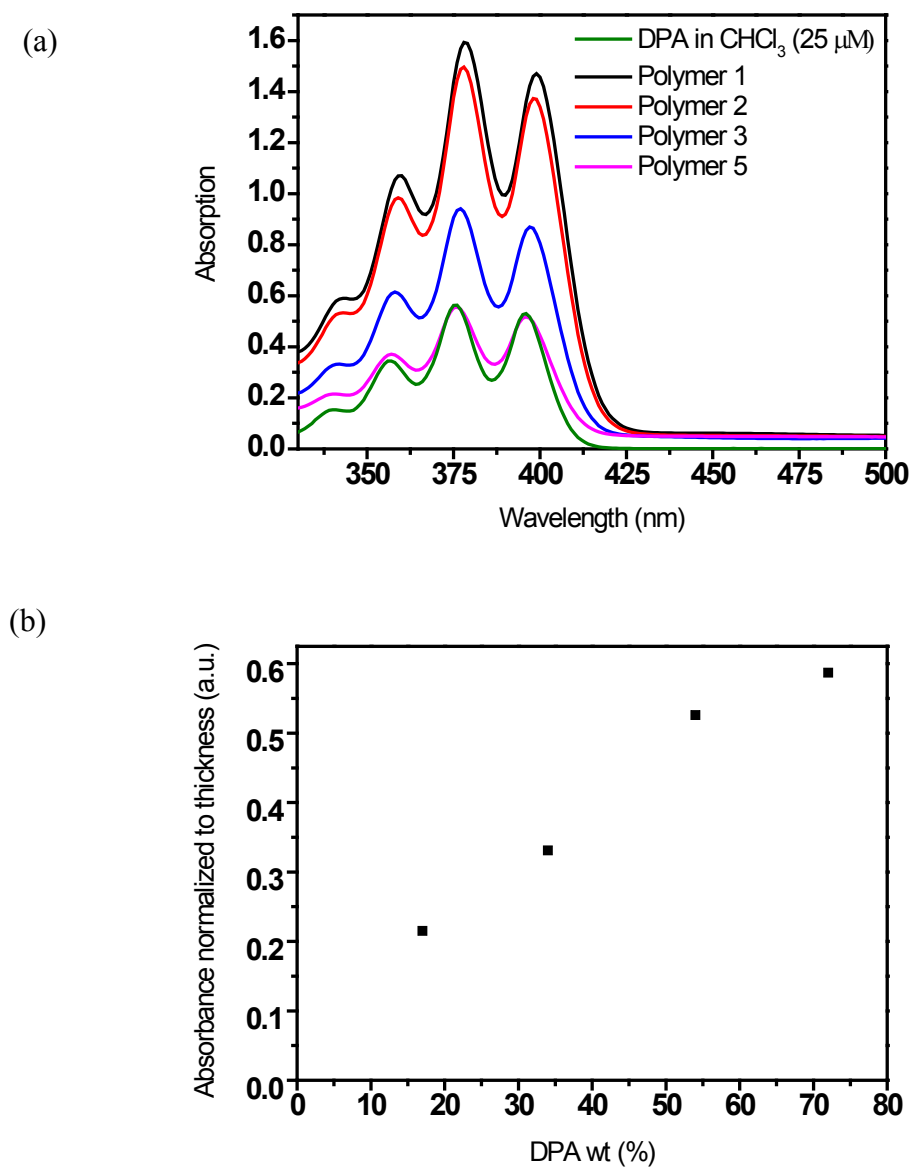


**Fig. S26** (a) Absorption spectra of the spin-coated (co)polymers films **1**, **2**, **3**, and **5**, compared to a reference solution of neat DPA dissolved in CHCl<sub>3</sub> (25 μM). (b) Absorbance at  $\lambda = 342$  nm extracted from the spectra in (a) plotted as a function of weight fraction of DPA in the polymers.

## V. Morphological characterization

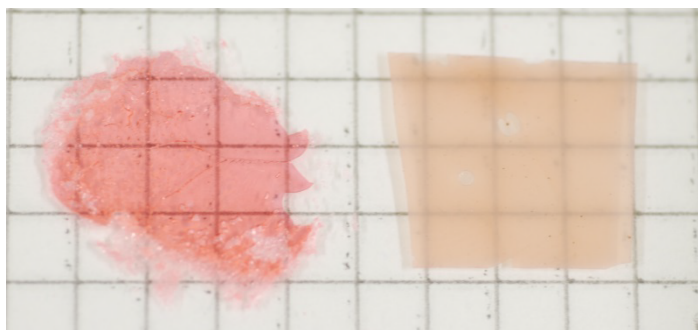


**Fig. S27** Picture of compression-molded film of copolymer **3** (containing 34 wt% DPA) with 0.05 wt% of PdOEP processed at 160 °C (left) and a PMMA blend with 34 wt% DPA and 0.05 wt% PdOEP processed at 240 °C (right). The phase separation of high DPA content from polymer matrix is vanished in copolymer film.

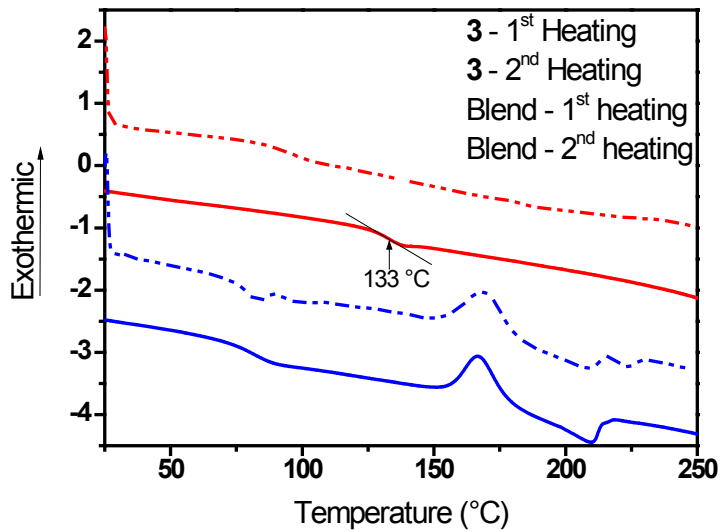


**Fig. S28** Differential scanning calorimetry (DSC) thermograms of a film of copolymer **3** (containing 34 wt% DPA) with 0.05 wt% of PdOEP (red curves) prepared by Method B and a PMMA blend with 34 wt% DPA and 0.05 wt% PdOEP processed at 240 °C (blue curves), recorded under nitrogen. Samples were first heated from 25 °C to 250 °C (dotted lines) and, after cooling to 0°C (not shown), heated again to 260 °C (solid lines), all with heating or cooling rates of 10 °C/min.

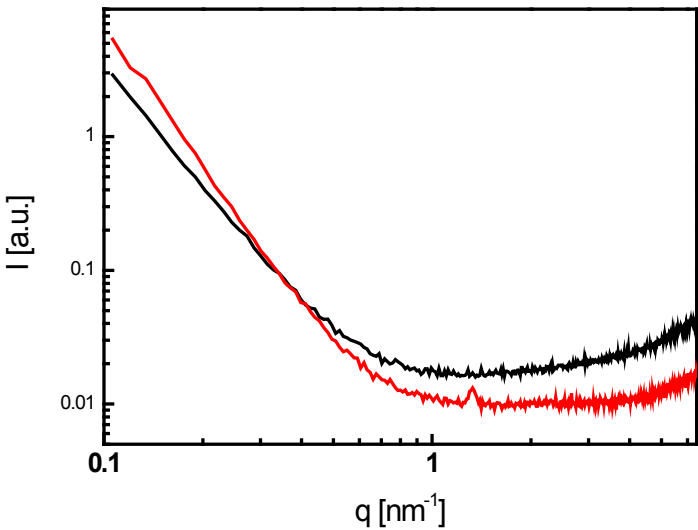


**Fig. S29** Small-angle X-ray scattering (SAXS) spectra of films of copolymers **3** (containing 34 wt% DPA, red curve) and **6** (8 wt% DPA, black), both films are doped with 0.05 wt% of PdOEP and prepared by Method B. The scattering curves do not exhibit any feature that could be related to a well-defined phase segregation. Instead, an apparent power like regime is present up to  $q = 2 \text{ nm}^{-1}$ , strongly indicating rather disordered structural heterogeneities, and on the corresponding length scale there is not sign of aggregation. The intensity upturn beyond  $q = 2 \text{ nm}^{-1}$  is related to the so-called amorphous halo.<sup>3,4</sup>

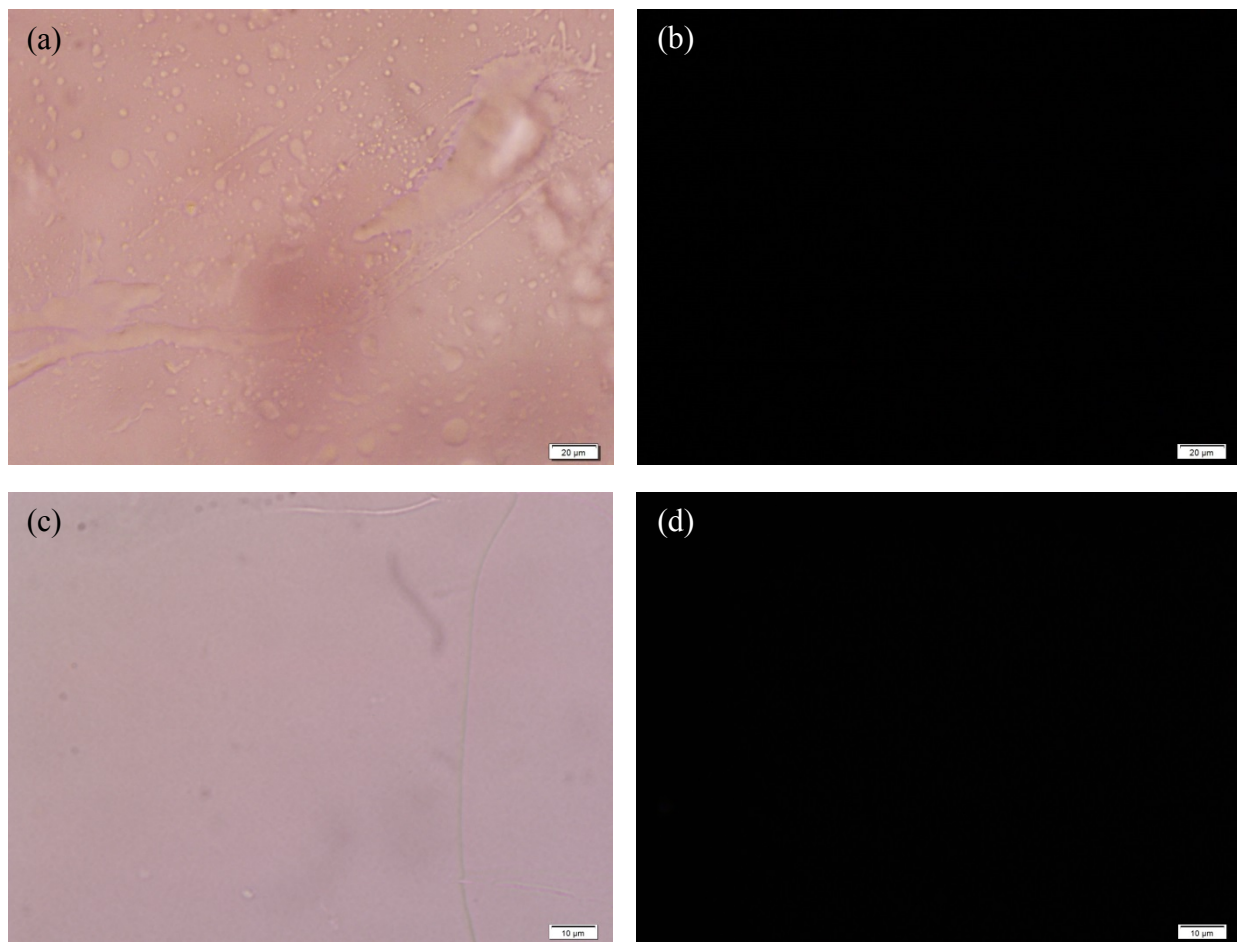


**Fig. S30** Optical micrographs of films of copolymers **3** (containing 34 wt% DPA) (a-b) and **6** (containing 8 wt% DPA) (c-d). Both films were prepared by Method B and are doped with 0.05 wt% of PdOEP. Pictures (a) and (c) were taken under parallel polarizers, while pictures (b) and (d) were taken under crossed polarizers. The scale bar corresponds to 20 µm (a-b) and 10 µm (c-d).

## VI. Optical measurements

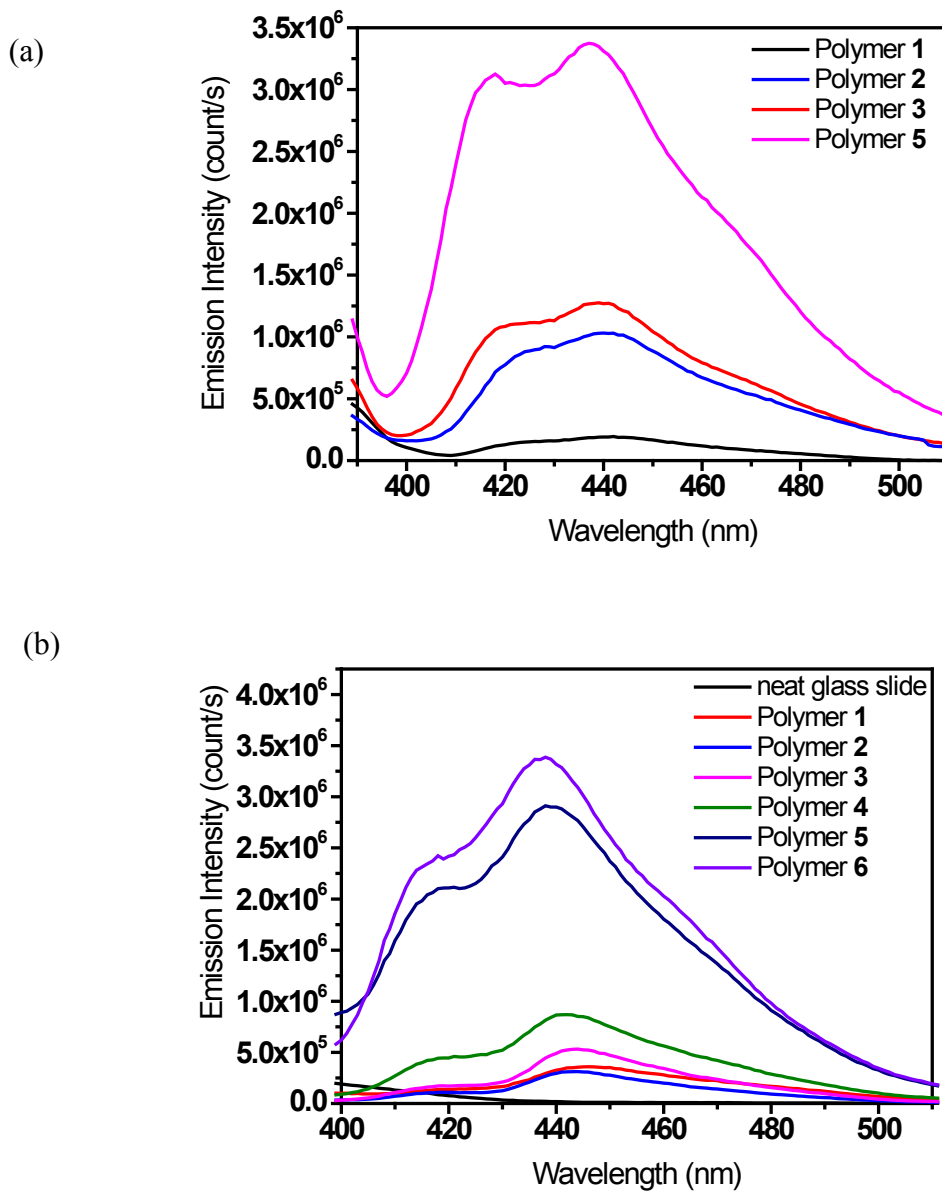


**Fig. S31** Fluorescence emission spectra of (a) spin-coated neat (co)polymers **1-3** and **5** and (b) upconverting films of (co)polymers, **1-6** doped with PdOEP (0.05 wt%) measured upon excitation with Xe arc lamp at 370 nm.

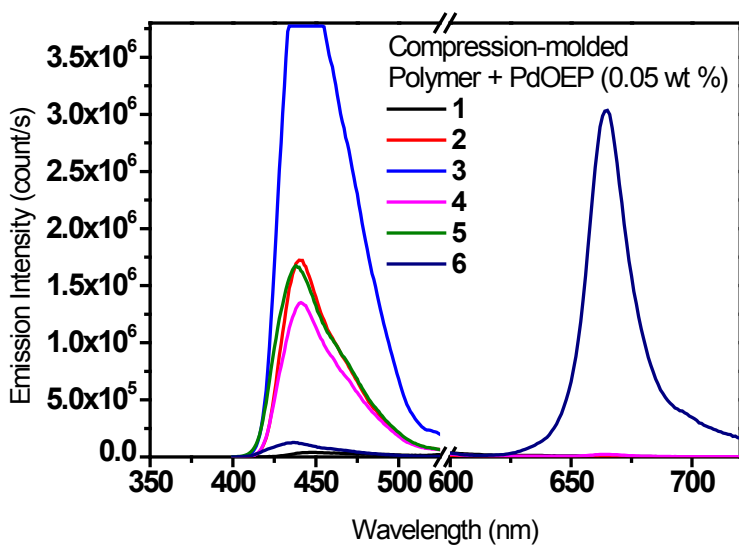


**Fig. S32** Emission spectra of compression-molded films comprising (co)polymers, **1-6** and 0.05 wt% of PdOEP upon irradiation with a laser at 543 nm. Delayed upconverted fluorescence was observed between 400-520 nm for all films. Phosphorescence was observed exclusively in case of the film of copolymer **6**.

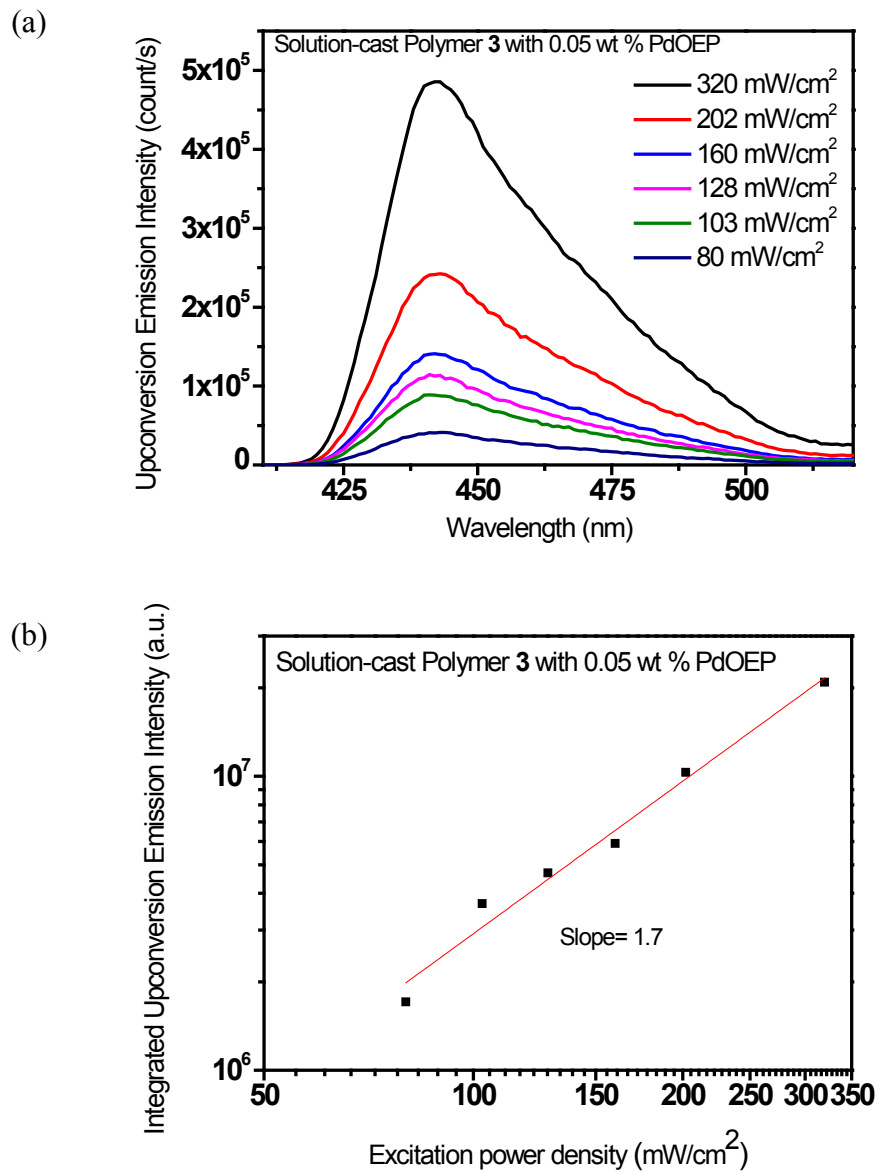


**Fig. S33** (a) Upconverted emission spectra of solution-cast (co)polymer films excited with HeNe laser at 543 nm with variation of the excitation power density from 80 mW/cm<sup>2</sup> to 320 mW/cm<sup>2</sup>. (b) Double logarithmic plots of the data shown in (a), and a least square fit of the data (slope = 1.7).

**Table S2** Maximum upconversion intensity in counts/s as a function of PdOEP and DPA content in wt%.

		wt% DPA					
		72	54	34	26	17	8
wt% PdOEP	0.03	--	--	1.85E+06	--	--	--
	0.05	--	0	7.8E+06	1.84E+07	1.17E+07	9.29E+06
	0.18	--	0	--	4.59E+06	3.43E+06	--
	0.4	--	--	--	--	9.86E+5	--
	0.7	1.96E+4	--	--	--	--	--

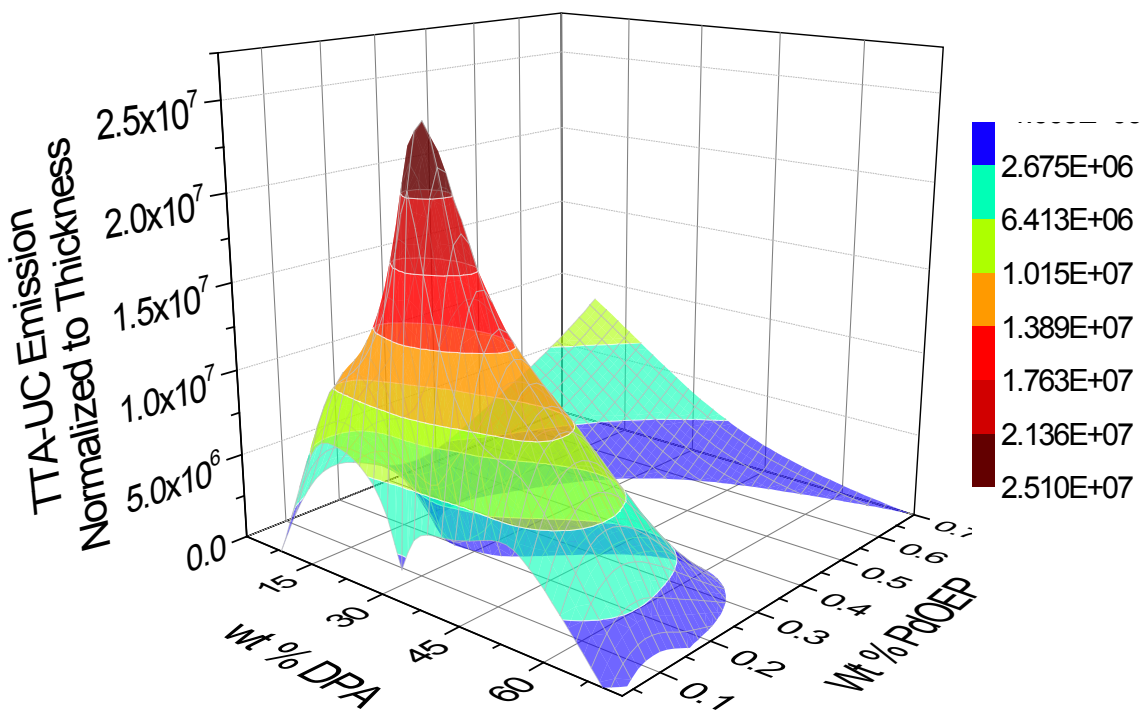


**Fig. S34** Upconversion intensity normalized to the thickness as function of wt% of PdOEP and DPA based on Table S2. The data was converted into a 3D matrix on Origin 8.5 using xyz Random Gaussian template which is based on Random (thin plate spline) gridding method with 50x50 grids and extrapolation. The resulting matrix was plotted in 3D color map surface without smoothing, and coordinating wt% DPA on x-axis, wt% PdOEP on y-axis and upconversion intensity normalized to thickness on z-axis.

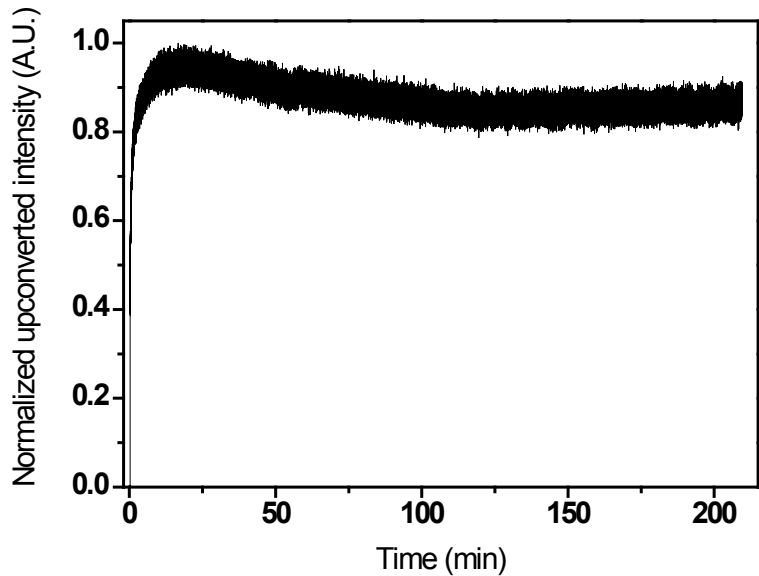


**Fig. S35** Normalized upconverted emission intensity of films of copolymer **3** and 0.05 wt% PdOEP upon continuous wave excitation at 543 nm ( $320 \text{ mW/cm}^2$ ), monitored at 445 nm. The sample was prepared with Method B and a stable upconversion intensity under ambient conditions found when measuring over the course of 3.5h.

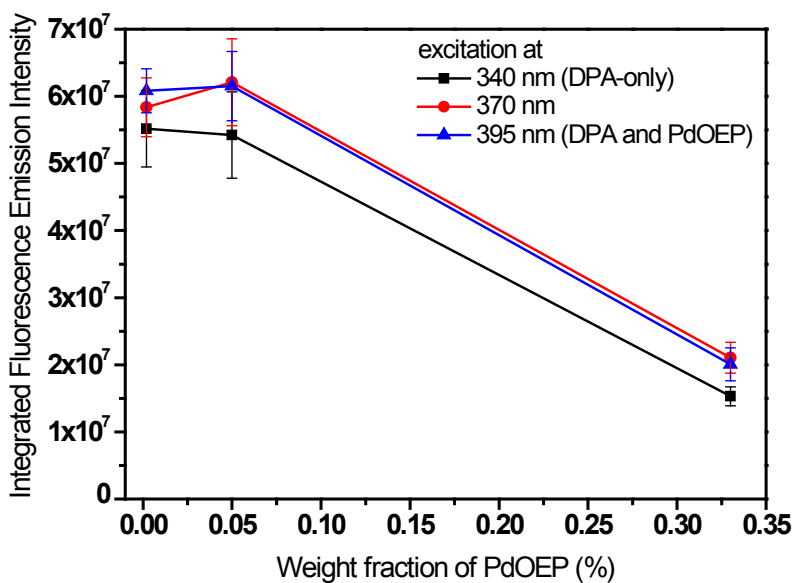


**Fig. S36** Integrated fluorescence emission intensity of compression-molded films based on blends of polymer **3** and 0.002, 0.05 or 0.33 wt% PdOEP upon excitation at 340 (only DPA), 370 and 395 nm (DPA and PdOEP). Every data point shows the average integrated intensity measured at four different spots.

For all the wavelengths monitored a significant decrease in fluorescence to ca. 1/3 intensity was found for the sample containing 0.33 wt% PdOEP, even when irradiating at 340 nm, efficiently absorbed by DPA only. Strong decrease of DPA-fluorescence regardless of the irradiated species (DPA or DPA and PdOEP) indicates formation of exciplexes or other non-radiative relaxation pathways induced by the presence of the sensitizer, e.g. energy transfer from the emitter to the sensitizer.

## References

1. W. Fudickar and T. Linker, *Chem-Eur J*, 2006, 12, 9276-9283.
2. T. G. Fox and P. J. Flory, *J. Appl. Phys.*, 1950, 21, 581-591.
3. N. Kasai and M. Kakudo, *X-Ray diffraction by macromolecules*, Springer, 2005.
4. U. W. Gedde, *Polymer physics*, Chapman&Hall edn., 1995.